Stanford Exploration Project, Report 113, July 8, 2003, pages 163–177

Improving the amplitude accuracy of downward continuation operators

Ioan Vlad, Thomas Tisserant, and Biondo Biondi[1]

ABSTRACT

While wave-equation downward continuation correctly accounts for traveltimes, the amplitude and phase of the image can be improved. We show concrete ways of implementing a previously proposed improvement using both mixed-domain and finite-difference extrapolators. We apply the corrections to constant velocity, constant vertical velocity gradient and $v(x,z)$ cases and show that the correction brings amplitudes closer to the theoretical values.

INTRODUCTION

While accurate kinematics are the first requirement of a useful seismic image, its amplitude and phase behavior are nonetheless important. The amplitude and phase information can be useful in wave-equation migration velocity analysis or as direct hydrocarbon indicators. The one-way wavefield extrapolators (Claerbout, 1971) employed in migration produce correct traveltimes. However, their amplitude and phase characteristics can be improved.

Zhang (1993) brings theoretical insight into the problem of improving the amplitudes of downward continuation operators. Zhang et al. (2001) compare them with Kirchhoff inversion and provide formulas for amplitude-preserving shot-profile migration that are accurate in the case of constant velocity. Along the same lines, Zhang et al. (2002) give an additional term for the case of velocity varying only with depth. Zhang et al. (2003a) extend the argument to heterogeneous media. Besides that, Zhang et al. (2003b) provide a more accessible description of the basic theory of the method. In this paper, we describe implementations of this amplitude-preserving downward continuation operators in the $\omega - x$ domain (finite-difference), as well as in the mixed domain.

ANALYTICAL FORMULATION

Denote the surface position vector by

$$\vec{x} = (x_1, x_2), \tag{1}$$

[1]**email:** nick@sep.stanford.edu, thomas@sep.stanford.edu, biondo@sep.stanford.edu

the temporal frequency by ω, and the velocity by

$$v = v(\vec{x}, z). \tag{2}$$

We define the operator Λ as

$$\Lambda = i\sqrt{\frac{\omega^2}{v^2} + \frac{\partial^2}{\partial x_1^2} + \frac{\partial^2}{\partial x_2^2}}, \tag{3}$$

and the operator Γ as

$$\Gamma = \frac{1}{2v}\frac{\partial v}{\partial z}\frac{1}{1 + \frac{v^2}{\omega^2}\left(\frac{\partial^2}{\partial x_1^2} + \frac{\partial^2}{\partial x_2^2}\right)}. \tag{4}$$

Without the amplitude correction, shot profile migration proceeds by computing the upward going and the downward going wavefields at all depths:

$$\left(\frac{\partial}{\partial z} - \Lambda\right) U = 0, \tag{5}$$

$$\left(\frac{\partial}{\partial z} + \Lambda\right) D = 0. \tag{6}$$

To solve these equations, we need boundary conditions (inputs into the downward continuation). The recorded shot gather is taken as the upper boundary condition for the upward going wavefield, and a Dirac, approximated by a small wavelet, is taken as the upper boundary condition for the downward going wavefield:

$$U(\vec{x}, z = 0, \omega) = FFT\left[\text{Shotgather}(\vec{x}, t)\right]_{(\omega)} \tag{7}$$

$$D(\vec{x}, z = 0, \omega) = FFT\left[\text{Shot}(\vec{x}, t)\right]_{(\omega)} = FFT\left[\delta(\vec{x} - \vec{x}_{shot}, t)\right]_{(\omega)} \tag{8}$$

The reflectivity image is produced using the imaging condition:

$$R(\vec{x}, z) = \sum_{\omega} \frac{U(\vec{x}, z, \omega)}{D(\vec{x}, z, \omega)}. \tag{9}$$

According to Zhang et al. (2003a), to improve the amplitude and phase of the image R, we only need to add the Γ operator into the downward continuation equations:

$$\left(\frac{\partial}{\partial z} - \Lambda - \Gamma\right) p_U = 0 \tag{10}$$

$$\left(\frac{\partial}{\partial z} + \Lambda - \Gamma\right) p_D = 0 \tag{11}$$

and while taking the same boundary conditions for the upward going wavefield, to apply a correction to the downward going wavefield boundary condition:

$$p_U(\vec{x}, z = 0, \omega) = FFT\left[\text{Shotgather}(\vec{x}, t)\right]_{(\omega)}, \tag{12}$$

$$p_D(\vec{x}, z = 0, \omega) = \frac{1}{2}\Lambda^{-1} FFT\left[\text{Shot}(\vec{x}, t)\right]_{(\omega)}. \tag{13}$$

The imaging condition remains the same:

$$R(\vec{x},z)=\sum_{\omega}\frac{p_U(\vec{x},z,\omega)}{p_D(\vec{x},z,\omega)}. \tag{14}$$

The only differences between the amplitude-preserving algorithm and the traditional one are the use of the Γ operator in downward continuation and the application of the Λ^{-1} operator to the shot boundary condition. In the following sections, we will describe implementations of the two operators in the $\omega-x$ domain (finite-difference), as well as in the mixed domain. We will also show 2-D synthetic examples of applying the operators.

IMPLEMENTING THE Λ^{-1} OPERATOR

Finite differences

We denote the source wavefield by $q(x,\omega)=FFT\left[\text{Shot}(\vec{x},t)\right]_{(\omega)}$. Equation (13) can be written:

$$p_D=\frac{1}{2i}\left(\frac{\omega^2}{v^2}+\frac{\partial^2}{\partial x^2}\right)^{-\frac{1}{2}}q. \tag{15}$$

We then take a Taylor expansion of Λ^{-1} by considering k_x small compared to $\frac{\omega}{v}$:

$$p_D\simeq\frac{iv}{2\omega}\left(-1+\frac{v^2}{2\omega^2}\frac{\partial^2}{\partial x^2}\right)q. \tag{16}$$

Explicit finite differences are used to obtain a numerical solution:

$$p_D^x = \frac{iv}{2\omega}\left[-q^x+\frac{v^2}{2\omega^2}\left(\frac{q^{x-1}-2q^x+q^{x+1}}{\Delta x^2}\right)\right] \tag{17}$$

$$= \frac{iv}{2\omega}\left[\Delta_3 q^{x-1}-(1+2\Delta_3)q^x+\Delta_3 q^{x+1}\right], \tag{18}$$

where $\Delta_3=\frac{1}{2}\left(\frac{v}{\omega\Delta x}\right)^2$.

Mixed domain

In a homogeneous media, $-i\Lambda=k_z=k_{z0}$. Hence the Λ^{-1} correction is simply a division by k_{z0} of the source wavefield at the surface. If a split-step formulation of $k_z=k_{z0}+\omega\left(\frac{1}{v}-\frac{1}{v_0}\right)$ is considered, then the corrections must be carried out both in the space and wavenumber domain. One solution consists of doing the following expansion:

$$\frac{1}{k_z}=\frac{1}{k_{z0}+\omega\left(\frac{1}{v}-\frac{1}{v_0}\right)}\simeq\frac{1}{k_{z0}}\left[1-\frac{\omega}{k_{z0}}\left(\frac{1}{v}-\frac{1}{v_0}\right)\right]. \tag{19}$$

It is now possible to perform the correction in a few stages in the space and wavenumber domain.

IMPLEMENTING THE Γ OPERATOR

Finite differences

Each of Equations (10) or (11) can be split in two parts:

$$\frac{\partial P}{\partial z} = \pm i k_z P \tag{20}$$

$$\frac{\partial P}{\partial z} = \frac{1}{2v}\frac{\partial v}{\partial z}\frac{1}{1+\frac{v^2}{\omega^2}\frac{\partial^2}{\partial^2 x}}P. \tag{21}$$

Equation (20) can be written in the general form of the 45° equation (Claerbout, 1999) in which α and β are two coefficients to be set:

$$\frac{\partial P}{\partial z} = \pm\frac{i\omega}{v}\frac{\alpha\frac{v^2}{\omega^2}\frac{\partial^2}{\partial^2 x}}{1+\beta\frac{v^2}{\omega^2}\frac{\partial^2}{\partial^2 x}}P. \tag{22}$$

Equation (21) resembles (22) enough for us to use the same scheme to solve it. We present some details of the implementation in Appendix A.

Mixed domain

One solution of (10) is:

$$P_z' = P_z e^{-\Gamma\Delta z} \tag{23}$$

$$P_{z+\Delta z} = P_z' e^{\mp\Lambda\Delta z}. \tag{24}$$

We implemented (24) with the split-step method (Stoffa et al., 1990). To implement (23) we take a Taylor expansion of the Γ term:

$$\Gamma = \frac{v_z}{2v}\frac{1}{1-\left(\frac{vk_x}{\omega}\right)^2} \simeq \frac{v_z}{2v}\left[1+\left(\frac{vk_x}{\omega}\right)^2+\left(\frac{vk_x}{\omega}\right)^4\right]. \tag{25}$$

Equation (23) becomes:

$$P_z' = P_z e^{-\frac{v_z\Delta z}{2v}} e^{-\frac{v_z\Delta z v k_x^2}{2\omega^2}} e^{-\frac{v_z\Delta z v^3 k_x^4}{2\omega^4}}. \tag{26}$$

The last exponentials cannot be computed in a single step because the velocity terms and the horizontal wavenumber do not belong to the same domain. One solution consists of expanding the exponentials in a Taylor series and keeping only the terms of order smaller or equal to 4 in k_x:

$$e^{-\frac{v_z\Delta z v k_x^2}{2\omega^2}} e^{-\frac{v_z\Delta z v^3 k_x^4}{2\omega^4}} \simeq 1-\frac{v_z\Delta z v}{2}\left(\frac{k_x}{\omega}\right)^2+\frac{v_z\Delta z v^2}{2}\left(\frac{v_z\Delta z}{4}-v\right)\left(\frac{k_x}{\omega}\right)^4. \tag{27}$$

The Γ correction is:

$$P_z' = P_z e^{-\frac{v_z\Delta z}{2v}}\left[1-\frac{v_z\Delta z v}{2}\left(\frac{k_x}{\omega}\right)^2+\frac{v_z\Delta z v^2}{2}\left(\frac{v_z\Delta z}{4}-v\right)\left(\frac{k_x}{\omega}\right)^4\right]. \tag{28}$$

We give an algorithm of the mixed-domain implementation in Appendix B.

RESULTS

To test the effect of the boundary condition correction operator we used a constant velocity ($1000m/s$) model, in which the Γ correction is zero. Because the correction only applies to the source wavefield, we did not go through the imaging condition. We generated a shot at the surface, downward propagated it until $z = 375m$, and then picked the maximum amplitudes at each x location at that depth. Figure 1 shows that the operator $\frac{1}{2}\Lambda^{-1}$ brings the amplitudes much closer to the analytically computed curve both for mixed domain and for finite difference. In the case of the mixed-domain method (top and middle panels), the amplitudes are practically as good as those obtained with two-way wave equation modeling. In the case of finite difference (bottom panel), artifacts interfere constructively and destructively with the true events and lead to amplitude variations along the hyperbola. However, even with artifacts, the corrected amplitudes are closer to the analytical ones than the uncorrected ones.

The Γ correction was tested the same way: by comparing the amplitudes from a shot, propagated until $z = 1125m$ in a $v = 1000m/s + 2z$ medium, for which amplitude curves could be computed analytically (Appendix C). The most meaningful comparison is with the WKBJ amplitude correction (Clayton and Stolt, 1981):

$$\text{WKBJ Correction Factor} = \sqrt{\frac{k_z(z = z_{max})}{k_z(z = 0)}} = \left(\frac{\frac{\omega^2}{v^2_{zmax}} - k_x^2}{\frac{\omega^2}{v^2_{z=0}} - k_x^2} \right)^{\frac{1}{4}} . \tag{29}$$

In $v(z)$ the Γ correction has the same effect as the WKBJ correction, but unlike it, it can also be applied in a $v(x,z)$ medium. The differences at large angles between the Γ and the WKBJ result can be attributed to the truncations in the Taylor expansions in the Γ term.

We then downward continued a shot until $z = 2000m$ through the velocity model shown in Figure 3. Downward continuation was performed with both split-step (left panels) and finite differences (right panels), without applying any correction (upper panels), with a Λ^{-1} boundary condition only (middle panels) and with both Λ^{-1} and Γ corrections (lower panels). The corrections result in phase changes and in a much more uniform repartition of amplitudes.

CONCLUSIONS

We have shown ways of implementing the amplitude corrections proposed by Zhang (1993) both by mixed-domain and by finite-difference methods. We applied them to media of constant velocity, constant vertical velocity gradient, and of laterally varying velocity. In constant velocity, and especially for split-step modeling, the boundary condition correction makes amplitudes comparable to the analytical ones, or to those obtained by two-way wave equation modeling. In the constant vertical velocity gradient medium, the Γ correction has the same effect as the WKBJ correction, but unlike it, it can also be applied in a $v(x,z)$ medium. Future work will include application of the same procedure to other laterally varying velocity models

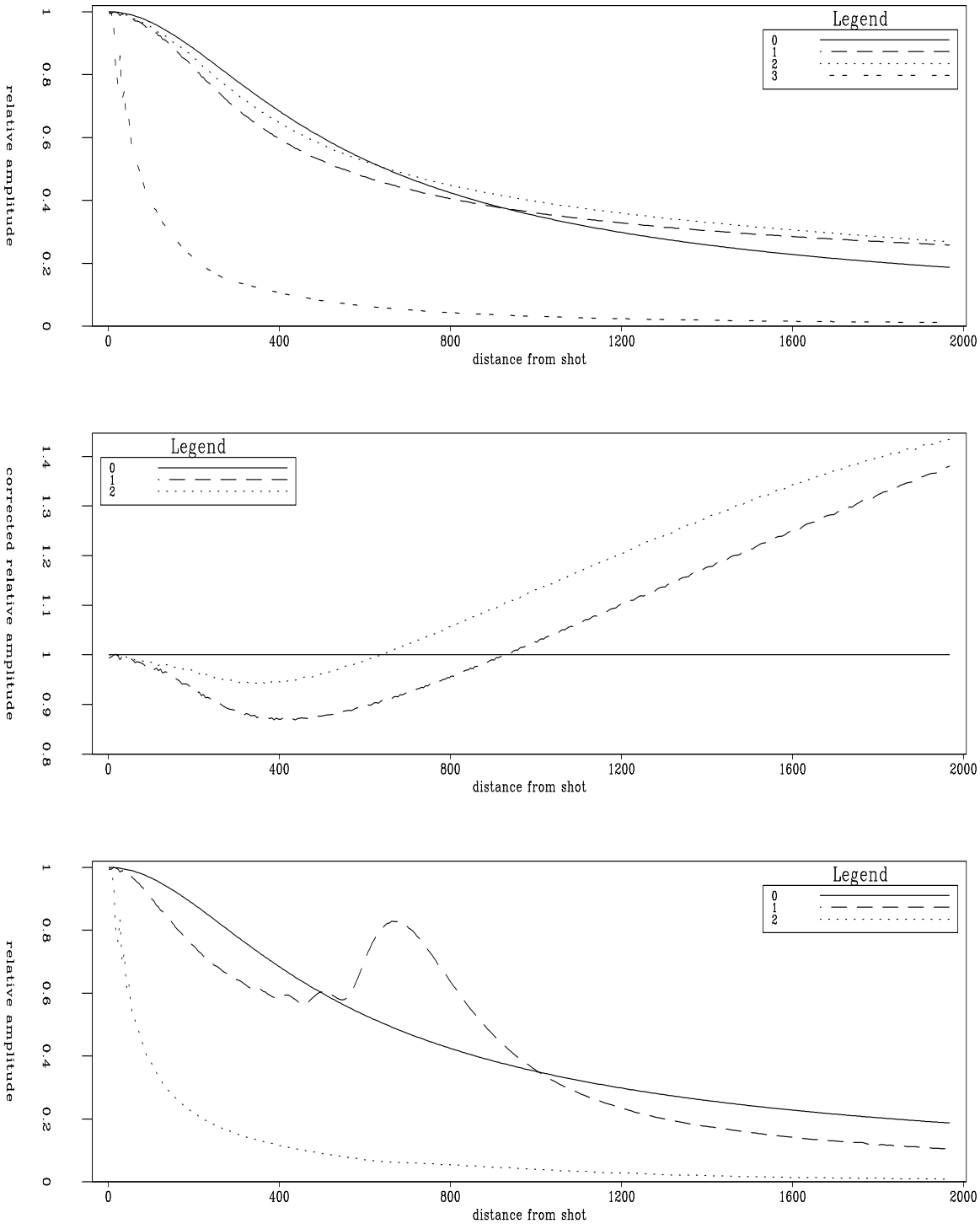

Figure 1: Amplitudes computed in the following ways: **Top panel -** `Curve 0:` analytically; `Curve 1:` mixed domain *with* Λ^{-1} correction; `Curve 2:` two-way wave equation modeling; `Curve 3:` mixed domain *without* Λ^{-1} correction. **Middle panel - normalized to the analytical curve:** `Curve 0:` analytically; `Curve 1:` mixed domain *with* Λ^{-1} correction; `Curve 2:` two-way wave equation modeling. **Bottom panel -** `Curve 0:` analytically; `Curve 1:` finite-difference *with* Λ^{-1} correction; `Curve 2:` finite-difference *without* Λ^{-1} correction. nick3-laminus [CR]

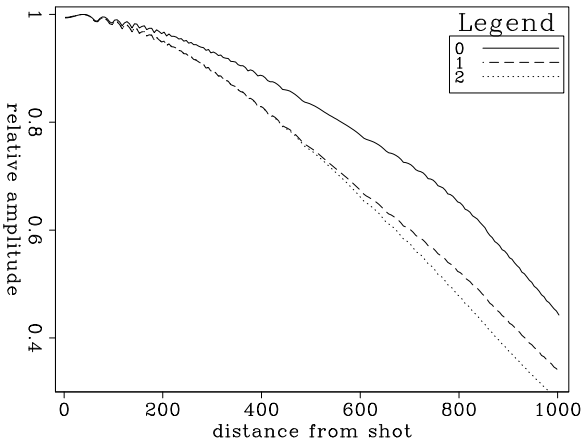

Figure 2: Amplitudes of a shot propagated by split-step, with the following corrections: **Curve 0:** Λ^{-1} correction only; **Curve 1:** Both Λ^{-1} and Γ corrections; **Curve 2:** Λ^{-1} and WKBJ corrections nick3-crscmp [CR]

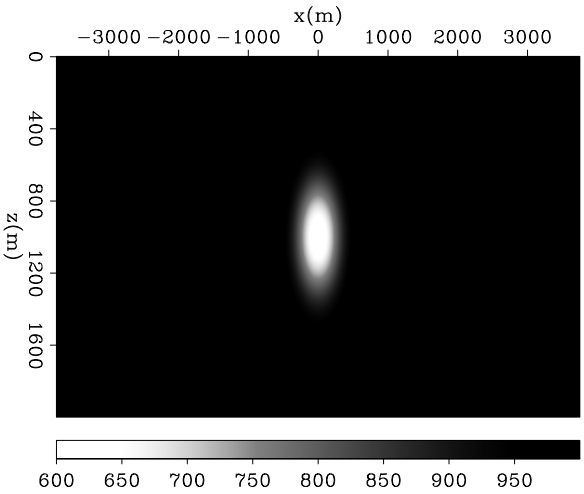

Figure 3: $V(x,z)$ velocity model nick3-symes_v [ER]

and to real data and validation of $v(x,z)$ results by comparison with results of ray-tracing with amplitudes.

ACKNOWLEDGMENTS

We thank Guojian Shan for his advice regarding finite differencing and for the two-way wave equation modeling program used for curve 2 in the top and middle panels of Figure 1, to Norm Bleinstein for bringing this topic to our attention during a recent visit to SEP, and to Bill Symes for the velocity model shown in Figure 3.

REFERENCES

Claerbout, J., 1971, Toward a unified theory of reflector imaging: Geophysics, **36**, no. 3, 467–481.

Claerbout, J. F., 1985, Imaging the Earth's Interior: Blackwell Scientific Publications.

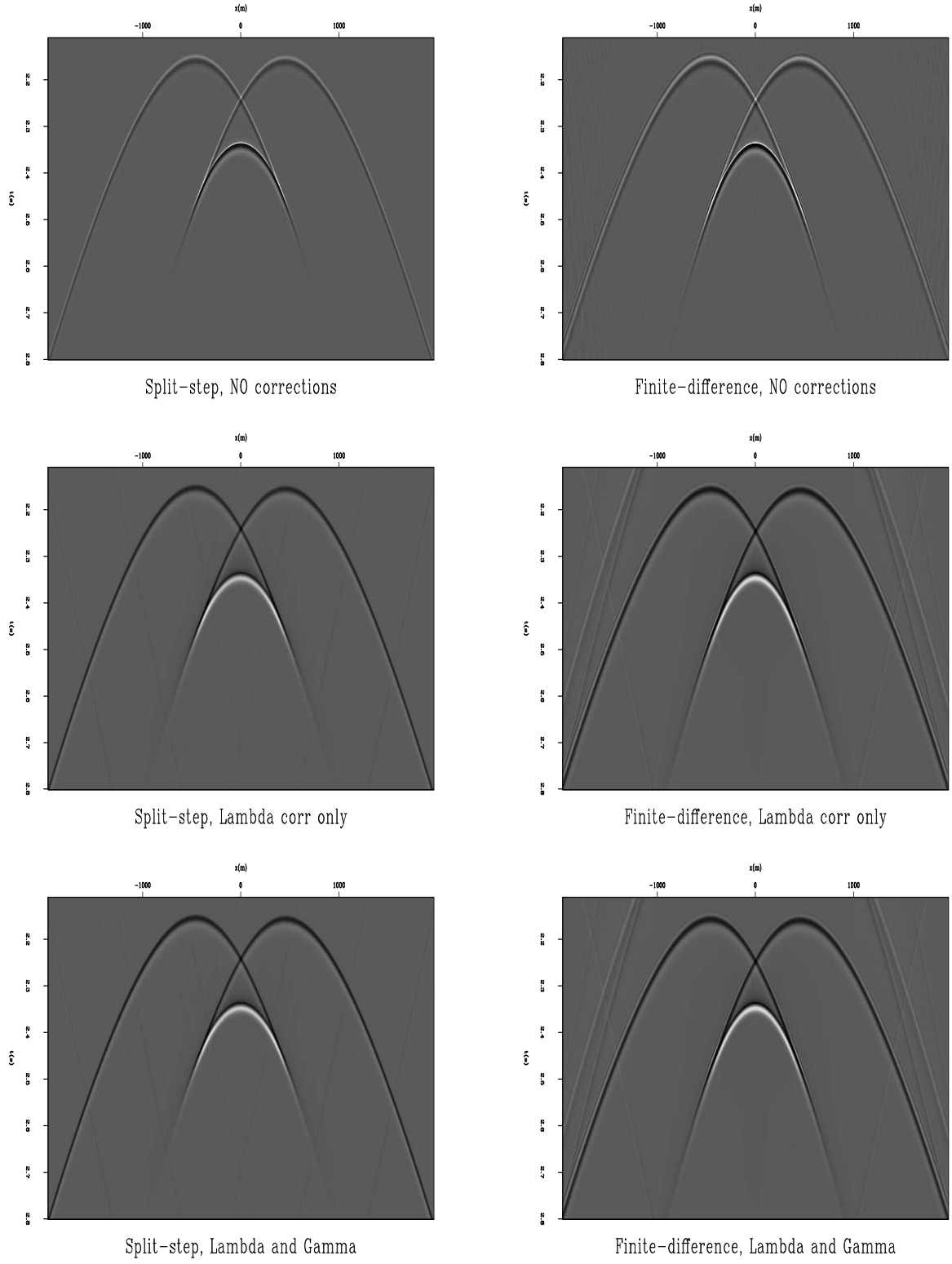

Figure 4: Wavefields of a shot propagated through the velocity model in Figure 3. **Left** panels: split-step; **Right** panels: finite difference; **Upper** panels: no amplitude correction; **Middle** panels: boundary condition correction (Λ^{-1}) correction only; **Lower** panels: both boundary condition (Λ^{-1}) and Γ correction. nick3-triptik [CR]

Claerbout, J. F., 1999, Basic earth imaging: Class notes, http://sepwww.stanford.edu/sep/prof/index.html.

Clayton, R. W., and Stolt, R. H., 1981, A Born-WKBJ inversion method for acoustic reflection data: Geophysics, **46**, no. 11, 1559–1567.

Fomel, S., and Claerbout, J. F., 1997, Exploring three-dimensional implicit wavefield extrapolation with the helix transform: SEP–**95**, 43–60.

Lee, M. W., and Suh, S. Y., 1985, Optimization of one-way wave equations: Geophysics, **50**, no. 10, 1634–1637.

Slotnick, M. M., 1936, On seismic computations, with applications, I: Geophysics, **1**, no. 1, 9–22.

Stoffa, P. L., Fokkema, J. T., de Luna Freire, R. M., and Kessinger, W. P., 1990, Split-step fourier migration: Geophysics, **55**, no. 04, 410–421.

Zhang, Y., Sun, J., Gray, S. H., Notfors, C., and Bleinstein, N., 2001, Towards accurate amplitudes for one-way wavefield extrapolation of 3-D common shot records: 71st Ann. Internat. Mtg., Soc. Expl. Geophys. (Workshop).

Zhang, Y., Sun, J., Gray, S. H., Notfors, C., Bleinstein, N., and Zhang, G., 2002, True amplitude migration using common-shot one-way wavefield extrapolation: 64th EAGE Annual Conference.

Zhang, Y., Zhang, G., and Bleinstein, N., 2003a, Theory of true amplitude common-shot migration: 65th EAGE Annual Conference.

Zhang, Y., Zhang, G., and Bleinstein, N., 2003b, Theory of true amplitude one-way wave equations and true amplitude common-shot migration: 65th EAGE Annual Conference.

Zhang, G., 1993, System of coupled equations for upgoing and downgoing waves: Acta Math. Appl. Sinica, **16**, no. 2, 251–263.

APPENDIX A

Solving equation 20 We define $n = \frac{v}{\omega}$. Equation 20 can be written:

$$\partial_z = \pm i \frac{\alpha n \partial_{xx}}{1 + \beta n^2 \partial_{xx}}, \tag{A-1}$$

or

$$\partial_z + \beta n^2 \partial_{xxz} \mp i \alpha n \partial_{xx} = 0. \tag{A-2}$$

We apply the finite difference method:

$$\partial_z p = \frac{1}{\Delta z}(p^x_{z+1} - p^x_z) \tag{A-3}$$

$$\partial_{xxz} p = \frac{1}{\Delta z \Delta x^2}(p^{x-1}_{z+1} - p^{x-1}_z) + \frac{-2}{\Delta z \Delta x^2}(p^x_{z+1} - p^x_z) + \frac{1}{\Delta z \Delta x^2}(p^{x+1}_{z+1} - p^{x+1}_z) \tag{A-4}$$

$$\partial_{xx} p = \frac{1}{\Delta x^2}(p^{x-1}_{z+1} - p^{x-1}_z) + \frac{-1}{2\Delta x^2}(p^x_{z+1} - p^x_z) + \frac{1}{\Delta x^2}(p^{x+1}_{z+1} - p^{x+1}_z). \tag{A-5}$$

After some little rearrangements, equation A-2 can be written:

$$\Delta p^{x-1}_{z+1} + (1 - 2\Delta)\, p^x_{z+1} + \Delta p^x_{z+1} = \Delta^* p^{x-1}_z + \left(1 - 2\Delta^*\right) p^x_z + \Delta^* p^x_z. \tag{A-6}$$

where

$$\Delta = \frac{\beta n^2}{\Delta x^2} \mp i \frac{\alpha n \Delta z}{2\Delta x^2} \tag{A-7}$$

For downward continuing the receiver (upgoing) wavefield, we choose the positive sign in the relation above; for downward continuation of the source (downgoing) wavefield we take the sign in Δ to be negative. To solve the 15° equation, $(\alpha, \beta) = (0.5, 0)$. For the 45° equation, $(\alpha, \beta) = (0.5, 0.25)$, and for the 65° equation, $(\alpha, \beta) = (0.478242060, 0.376369527)$ (Lee and Suh, 1985). In our implementation, we have used the 65° equation with the "$\frac{1}{6}$ trick" (Claerbout, 1985) for improving the accuracy of the second derivative. This changes (A-2) and (A-7) into

$$\partial_z + \left(\beta n^2 + \frac{\Delta x^2}{s}\right) \partial_{xxz} \mp i \alpha n \partial_{xx} = 0 \tag{A-8}$$

$$\Delta = \left(\frac{\beta n^2}{\Delta x^2} + \frac{1}{s}\right) \mp i \frac{\alpha n \Delta z}{2\Delta x^2} \tag{A-9}$$

where we took $s = 8.13$ (Fomel and Claerbout, 1997). Equation (A-6) with the new Δ gives a tridiagonal system for each frequency and depth.

Solving equation 21

Equation (21) can be written:

$$\partial_z = \frac{v_z}{2v} \frac{1}{1 + n^2 \partial_{xx}}. \tag{A-10}$$

As for Equation (A-2), we use a Crank-Nicolson scheme for the second derivative in x. Equation (A-10) becomes:

$$\Delta_1 p_{z+1}^{x-1} + (1 - 2\Delta_1 + \Delta_2)\, p_{z+1}^{x} + \Delta_1 p_{z+1}^{x} = \Delta_1 p_{z}^{x-1} + (1 - 2\Delta_1 - \Delta_2)\, p_{z}^{x} + \Delta_1 p_{z}^{x} \quad \text{(A-11)}$$

where

$$\Delta_1 = \frac{n^2}{\Delta x^2}, \quad \text{(A-12)}$$

$$\Delta_2 = -\frac{v_z \Delta z}{4v}. \quad \text{(A-13)}$$

Equation (A-11) is solved the same way as (A-6).

APPENDIX B

We provide here the algorithm of our mixed-domain implementation of both Λ^{-1} and Γ corrections. The notations refer to a single spatial axis, but they can be easily extended to two axes. The Λ^{-1} correction is only applied to the source wavefield, and is only applied once, at the surface, not for each depth step. The correction is $P_{z=0} = -\frac{1}{2ik_z} Q$. Because it generates strong wraparound that translates as noise in the final image, it is recommended to pad the data with zeros, apply the correction, then window it to a smaller size for downward continuation.

For each frequency, to downward continue one step with corrected amplitudes (Γ operator) we Fourier transform to the wavenumber domain:

- $P_z(k_x) \leftarrow P_z(x)$.

In the wavenumber domain, we perform the following operations:

- Phase shift (part of split-step): $P^0_{z+\Delta z} \leftarrow e^{ik_{z0}\Delta z} P_{z+\Delta z}$
  where $k_{z0} = \sqrt{\frac{\omega^2}{v_0^2} - k_x^2}$, in which v_0 is the reference velocity at that depth.
- First order amplitude correction (part of Γ): $P^1_{z+\Delta z} \leftarrow \left(\frac{k_x}{\omega}\right)^2 P^0_{z+\Delta z}$.
- Second order amplitude correction (part of Γ): $P^2_{z+\Delta z} \leftarrow \left(\frac{k_x}{\omega}\right)^4 P^0_{z+\Delta z}$.

Three separate Fourier transforms are needed to transform back to the spatial domain:

- $P^0_{z+\Delta z}(x) \leftarrow P^0_z(k_x)$,
- $P^1_{z+\Delta z}(x) \leftarrow P^1_z(k_x)$,
- $P^2_{z+\Delta z}(x) \leftarrow P^2_z(k_x)$.

In the spatial domain we perform:

- First order amplitude correction (part of Γ): $P^1_{z+\Delta z} \leftarrow -\frac{v_z v \Delta z}{2} P^1_{z+\Delta z}$,
- Second order amplitude correction (part of Γ): $P^2_{z+\Delta z} \leftarrow \frac{v_z \Delta z v^2}{2}\left(\frac{v_z \Delta z}{4} - v\right) P^2_{z+\Delta z}$,
- Summation of all terms: $P_{z+\Delta z} \leftarrow e^{-\frac{v_z \Delta z}{2v}}\left(P^0_{z+\Delta z} + P^1_{z+\Delta z} + P^2_{z+\Delta z}\right)$,
- Split step: $P_{z+\Delta z}(x) \leftarrow e^{i\omega\left(\frac{1}{v}-\frac{1}{v_0}\right)\Delta z} P_{z+\Delta z}(x)$.

The Γ correction for the receiver wavefield is computed the same way. Once both wavefields have been computed, the imaging condition (9) is applied for each depth.

In laterally varying velocity the terms in the spatial wavenumber domain that contain k_x do not commute with terms that contain functions of x, namely v and v_z. We took care to apply the terms in the right order inside the Γ operator. Outside Γ, things change. Strictly mathematically speaking, Γ does not commute with the split-step, and the right order of applying the operators remains to be studied. As in the case of split-step (for which the two terms that compose it do not commute with each other either), the differences in output may not warrant the cost of the extra Fourier transforms.

APPENDIX C

At depth z and at each point x we compute:

$$I_x = \frac{A_0}{A_x} I_0, \tag{C-1}$$

where A_0 and A_x are the areas of the unitary wavefront and a particular wavefront respectively. For spherical wavefronts,
In 2-D: $A_0 = 2\pi R_0 = 2\pi$, $A_x = 2\pi R$ hence $I_x = \frac{1}{R} I_0$.
In 3-D: $A_0 = 4\pi R_0^2 = 4\pi$, $A_x = 4\pi R^2$ hence $I_x = \frac{1}{R^2} I_0$.
To be able to compute the perturbed amplitude I_x from the unitary amplitude I_0, we need to compute R, the radius of the spherical wavefront. Two cases where the wavefronts are spherical are media of constant velocity and constant vertical velocity gradient.

Constant velocity media In this simple case, the length of the ray is:

$$R = \sqrt{x^2 + z^2}. \tag{C-2}$$

Constant vertical velocity gradient media Let us consider a velocity field of the form $v = v_0 + az$, where a is a constant. Both the ray and the wavefront are circles as illustrated in Figure C-1. If the ray from a source located at the origin surfaces at $(x_{out}, 0)$, then according to Equation (15) in Slotnick (1936), the depth of penetration of the ray is:

$$z_0 = \frac{v_0}{a}\left[\sqrt{1+\left(\frac{ax_{out}}{2v_0}\right)^2} - 1\right]. \tag{C-3}$$

The ray takes the time $2t$ to travel from origin to $(x_{out}, 0)$, and only half of that – t – to get to

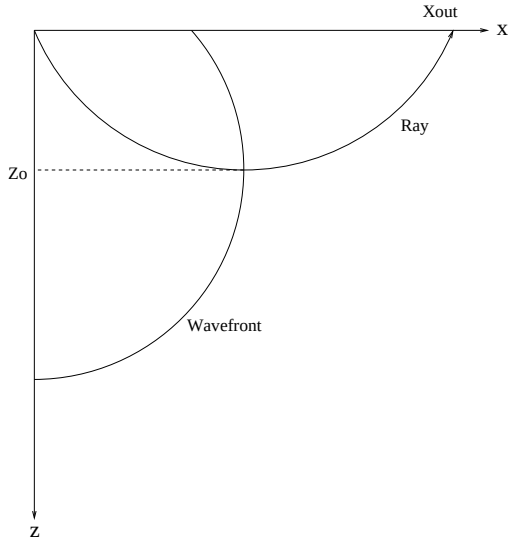

Figure C-1: Geometry of a wavefront and a ray in a constant vertical velocity gradient media. nick3-wavefront [NR]

the maximum depth point $(\frac{x_{out}}{2}, z_0)$. According to Equation (14) in Slotnick (1936),

$$t = \frac{1}{a}\sinh^{-1}\left(\frac{ax_{out}}{2v_0}\right). \tag{C-4}$$

Because wavefronts are orthogonal to rays, and because the ray is horizontal at the location where it reaches penetration depth, the equation of the only wavefront that passes through $(\frac{x_{out}}{2}, z_0)$ is:

$$x^2 + (z - z_0)^2 = \left(\frac{x_{out}}{2}\right)^2. \tag{C-5}$$

By plugging (C-3) and (C-4) into (C-5) we get the general equation of a wavefront:

$$x^2 + \left[z - \frac{v_0}{a}\left(\sqrt{1+\sinh^2(at)} - 1\right)\right]^2 = \left[\frac{v_o}{a}\sinh(at)\right]^2 = R^2. \tag{C-6}$$

There is a single ray that departs from the origin and arrives at the point (x, z). Its ray parameter is p and the time it takes to get to (x, z) is the solution of the integral in Equation (8) of Slotnick (1936) for the particular case of $v = v_0 + az$:

$$t = \frac{1}{a} \log F, \tag{C-7}$$

where we use the notation

$$F = \left(1 + \frac{az}{v_0}\right) \frac{1 + \sqrt{1 - p^2 v_0^2}}{1 + \sqrt{1 - p^2 (v_0 + az)^2}}. \tag{C-8}$$

We can write p as a function of x and z by writing Equation (12) in Slotnick (1936) as:

$$p^2 = \frac{1}{v_0^2 + \left[\frac{\frac{a}{2}(x^2 + z^2) + z v_0}{x}\right]^2}. \tag{C-9}$$

By combining (C-6) and (C-7) we can write R as a function of p instead of t:

$$R = \frac{v_0}{2a} \left(F - \frac{1}{F}\right). \tag{C-10}$$

To compute the wavefront radius R as a function only of x, z, v_0 and a, we have to plug (C-9) into (C-8), and then (C-8) into (C-10).